Analyzing the Performance of AC Microgrids in Stand-Alone Operation with Artificial Neural Network Controllers

Author(s): Ullah, Qudrat; Razmi, Peyman; Resende, Ĉnio Costa; Simões, Marcelo Godoy

Title: Analyzing the Performance of AC Microgrids in Stand-Alone Operation with Artificial Neural Network Controllers

Year: 2024

Version: Accepted manuscript

Please cite the original version:

Ullah, Q., Razmi, P., Resende, Ĉ. C. & Simões, M. G. (2024). Analyzing the Performance of AC Microgrids in Stand-Alone Operation with Artificial Neural Network Controllers. *2024 International Workshop on Artificial Intelligence and Machine Learning for Energy Transformation (AIE),* 1-6. IEEE. https://doi.org/10.1109/AIE61866.2024.10561255

Analyzing the Performance of AC Microgrids in Stand-Alone Operation with Artificial Neural Network Controllers

Qudrat Ullah [1*], Peyman Razmi[1], Ênio Costa Resende [1,2], Marcelo Godoy Simões[1]
[1]School of Technology and Innovations University of Vaasa, Vaasa, Finland,
[2]Faculty of Electrical Engineering, Federal University of Uberlandia, Uberlandia, Brazil

***Abstract*—The emergency of renewable resources-based power generation depends on the development of voltage source inverters to interface wind or solar power plants. The accurate functioning of these inverters, in turn, depends on the robust control systems capable of keep the inverters operational point in stable conditions even after non-controllable electrical contingencies. In this sense, literature has proposed the application of artificial intelligence algorithms to guarantee control robustness, however, it still lacks a detailed analysis for the application of Artificial Neural Networks (ANN) to replace linear controllers in microgrid (MG) environment. Given this theoretical frame, the main contribution of this work is to analyze ANN performance for the control of stand-alone inverters that work without the presence of the main grid. The proposed ANN-based control scheme will be is tested for stand-alone MG under different load conditions. The results obtained demonstrate the control strategy's effectiveness in managing abrupt load transitions and simulation results also exhibit that voltage or current THD is 0.71 % which makes it suitable for VSIs based MGs.**

***Index Terms*—Microgrid, Grid forming, Inverter, Stand alone, Artificial neural network**

I. Introduction

THE emergence of renewable energy resources paves the way for a profound shift in humankind's relationship with the concept of power generation. As these technologies gradually replace traditional fossil fuel-based power plants, they facilitate the mitigation of global warming effects by reducing CO_2 emissions. Depending on the large-scale production of various products and services for functionality, they can create numerous job positions. Diversifying the energy matrix ensures greater reliability for the energy system [1]. However, to realize their maximum social, environmental, and economic potential, renewable resources need to be connected to inverter devices for integration with the main grid or for stand-alone operation [2]. Inverters are electronic devices that convert DC voltage or current into AC through the switching of semiconductors [3]. Their functioning principle relies on Feedback Control (FC). In FC, the sensed variable is compared with a reference value, generating an error signal. This error signal is then sent to a controller loop that works to minimize the difference between the actual and desired values [4]. The mitigation of the error can be achieved through various control strategies. One of the simplest methods for controlling a static converter is the use of a Proportional Integral (PI) controller.The PI controller can be applied to control the DC-DC boost stage or the DC-AC conversion stage [5]. The DC-DC boost stage typically involves a boost converter that regulates the input voltage to achieve the maximum power point of the renewable resource [6]. In relation to the DC-AC stage, PI controllers are employed in series with the Park Transform [7]. Park transformation converts the ABC system of voltages in a dq rotating frame [8]. Other linear control strategies employed in static converters are the PID [9] and the Proportional Resonate (PR) [10], [11]. However, to improve performance and reach greater reliability and robustness, some authors replace the traditional linear controls by artificial intelligence techniques [12]. In [13], for instance, the use of a fuzzy logic classifier is proposed to control an autonomous voltage source inverter (VSI). The system is submitted to different -switching events, such as motor, non-linear loads, and capacitor banks. The obtained results demonstrated a better transient response for all the analyzed cases when compared to linear control strategies. In [14], in turn, the possibility of applying a regression tree algorithm in parallel with a droop controller to perform power management in an islanded MG is studied. The simulation experiments conducted in MATLAB/Simulink show the effectiveness of the regression tree machine learning algorithm over the PI controller in terms of the step response and harmonic distortion of the system. Artificial Neural Networks (ANN) are also employed for VSI inverter control [15], [16]. A neural network is a data processing system consisting of a large number of simple, highly interconnected processing elements in an architecture inspired by the structure of the cerebral cortex portion of the brain [17]. The network processes information by propagating it through the layers, with each neuron in one layer connected to several neurons in the next layer. The connections between neurons are associated with weights that adjust as the network learns from data, optimizing the ANN's performance in tasks such as classification, regression, and pattern recognition. In [18] it is proposed a comparative study in which a ANN-PI controller is employed in a VSI inverter, reaching better results than the Model Predictive Control (MPC) and hysteresis. However, the paper only considers the stand-alone operation and does not analyze the performance of the control

*Qudrat Ullah (e-mail: qudrat.ullah@uwasa.fi).
Peyman Razmi (e-mail: peyman.razmi@uwasa.fi).
Ênio Costa Resende (e-mail: enio.costaresende@uwasa.fi).
Marcelo Godoy Simões (e-mail: marcelo.godoy.simoes@uwasa.fi)

strategy under multi-inverter conditions. ANN is also applied for inverter control in [19], [20]. However, [19] refers only to single-phase inverters, and [20] addresses a single-phase modified packed U-cell five-level inverter, not considering the operation of 2 three-phase inverters in the stand-alone MG. For the revised literature, it is possible to notice a lack of works addressing the application of ANN to islanded MG control, because ANNs can be used for their ability to model complex patterns in data effectively because of their versatility, learning capability, and customization, and ANNs are powerful tools for tasks that involve understanding complex patterns and making predictions based on large amounts of data which is not possible using traditional controllers. In this sense, the main contribution of this work is to evaluate the application of ANN to perform controlling tasks of a stand-alone VSIs or in a MG formed by two three-phase inverters. The obtained results demonstrate the validity of the proposed ANN-based controller and the capability to guarantee stable and low distorted voltage even after load transition. Finally, this paper is organized as follows: Section II demonstrates the system description in detail; Section III explains both the PI and the ANN-based strategy of controlling; Section IV presents the simulation results and discussions for stand-alone VSIs in a MG operation; and finally Section V present conclusions about the obtained results.

II. SYSTEM DESCRIPTION

A. *Modeling of Grid forming Inverter*

The VSIs are required to maintain stable voltage in stand-alone/islanded or autonomous operating modes. Since stand-alone mode does not have an external grid, so VSIs are imperative here because of their role in facilitating the conversion of voltages from DC to AC voltages. This transformation procedure is accomplished with the help of particular control mechanisms of switching devices (MOSFETs or IGBTs) of VSIs, which are considered as the cornerstone in these emerging VSI systems. It consists of three legs, each leg having two switch tubes. These switch tubes are power devices consisting of IGBT along with inverse shunt diodes. The IGBT switches operate in complementary ways. The three-phase AC voltages or currents are produced at an angle of 120 from each phase. A DC voltage source is connected to the input side of the three-phase VSI, and loads are connected to the output side of the inverter and the LC filter is necessary in generating smooth output voltage, minimizing harmonics produced while switching of IGBTs of inverters and is mandatory for enhancing voltage stability. The proposed three-phase VSI and its control strategy under study is shown in Fig. 1. There are eight possible switching states for three legs of three phase VSI as provided in Table I. It is possible to determine the voltage between each leg of VSI and a point N by multiplying the voltages at the DC link (V_{in}) and the present switching state of the corresponding leg of VSIs. The voltage for an individual leg of VSI and any other point N can be determined by the multiplication of DC link voltage and existing switching state of the correlated leg of VSIs as can be seen in Equations (1), (2), and (3) [21].

$$V_{aN} = S_a \times V_{in} \tag{1}$$

$$V_{bN} = S_b \times V_{in} \tag{2}$$

$$V_{cN} = S_c \times V_{in} \tag{3}$$

The switching action of VSIs is responsible for introducing harmonics in the output voltage. These harmonics are responsible for producing low-quality power, and thus, LC filters are necessary to suppress these harmonics in the output of VSI. The voltages for each phase of VSI are obtained from line voltages using Equation (4), and finally, phase voltages are obtained from Equation (4) as mentioned in Equation (5), Equation (6) and Equation (7):

$$\begin{bmatrix} V_{ab} \\ V_{bc} \\ V_{ca} \end{bmatrix} = \begin{bmatrix} V_{aN} - V_{bN} \\ V_{bN} - V_{cN} \\ V_{cN} - V_{aN} \end{bmatrix} \tag{4}$$

$$V_{aN} = \frac{2}{3}V_{ab} + \frac{1}{3}V_{bc} \tag{5}$$

$$V_{bN} = -\frac{1}{3}V_{bc} - \frac{1}{3}V_{ab} \tag{6}$$

$$V_{cN} = -\frac{2}{3}V_{bc} - \frac{1}{3}V_{ab} \tag{7}$$

The equivalent series resistance of the inductor is denoted by r_L in Fig. 1. Thus, a properly designed LC filter of three-phase VSI helps in improving power quality, compliance with grid standards, and reliable operation of different types of connected loads at the output side. The filter current, output voltages and current for three-phase VSI are denoted by I_L, V_{out} and I_{out}, respectively. Equations (8) and (9) provide the dynamic behavior of the LC filter.

TABLE I: POSSIBLE SWITCHING CONFIGURATIONS

No.	S_a	S_b	S_c	Space Vector
1	0	0	0	$\overrightarrow{V_0}$
2	1	0	0	$\overrightarrow{V_1}$
3	1	1	0	$\overrightarrow{V_2}$
4	0	1	0	$\overrightarrow{V_3}$
5	0	1	1	$\overrightarrow{V_4}$
6	0	0	1	$\overrightarrow{V_5}$
7	1	0	1	$\overrightarrow{V_6}$
8	1	1	1	$\overrightarrow{V_7}$

$$C\frac{dV_{\text{out}}}{dt} = I_L - I_{\text{out}} \tag{8}$$

$$L\frac{dI_L}{dt} = V_z - V_{\text{out}} - I_L r_L \tag{9}$$

The eight permissible voltage vectors of VSI are represented by Vz, which is given in Table 1. By applying KCL and KVL on the individual VSI, the state space equations of individual VSI can be written as [21]:

$$\frac{dx}{dt} = Ax + By \tag{10}$$

For three-phase VSIs, the values for x, y, A and B are defined as:

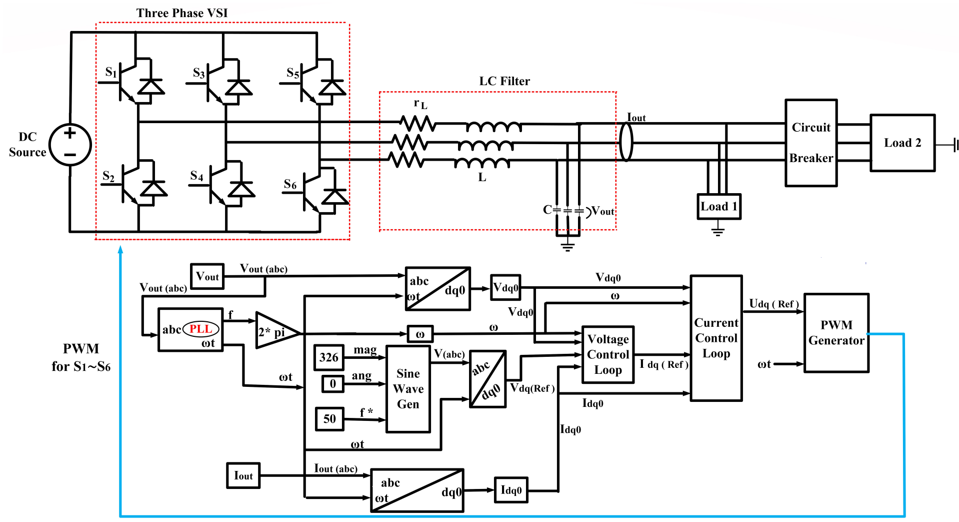

Fig. 1: Overview of proposed control scheme for standalone VSI

$$x = \begin{bmatrix} V_{\text{out}} \\ I_L \end{bmatrix}, \quad y = \begin{bmatrix} V_z \\ I_{\text{out}} \end{bmatrix}, \quad A = \begin{bmatrix} 0 & \frac{1}{C} \\ -\frac{1}{L} & -r_L \end{bmatrix} \tag{11}$$

$$B = \begin{bmatrix} 0 & 0 \\ \frac{1}{L} & 0 \end{bmatrix}$$

III. Control of Gridforming Inverter for Data Curation

Initially, the output voltages of VSIs are converted into Per unit (P.U) values. The obtained P.U value of output voltages is fed to phase locked loop (PLL). The PLL gives angle information which is used for coordinate conversions and angular frequency (inverter's electrical frequency). The synchronization from PLL is vital for precise conversion of references as well as measurements among the abc and dq0 reference frames. At the same time, the measured output current and voltage are converted into dq0 rotating frame. This conversion simplifies the controller design and makes easier to control them in a rotating frame like DC quantities instead of three-phase quantities. The measured output voltage and current in dq0 frame can be represented by Vdq and Idq respectively. After this, reference voltage in dq0 reference frame is generated with the help of system frequency and desired output voltage. The voltage and control loop of this control scheme is formulated consisting of cascaded PI controllers. The data curation is performed on both loops to obtain data for artificial function-fitting neural networks. In this context, a quintessential structure like Multilayer Perceptron (MLP) within the domain of Artificial Neural Networks (ANN) is deeply rooted in the pursuit of mirroring the learning processes of the human brain. MLPs consist of several layers of nodes in a directed graph, each layer being fully connected to the next. This includes an input layer, one or more hidden layers, and an output layer. Theoretically, MLPs are eminent for their capability to effectively approximate any continuous function, a property recognized as the universal approximation theorem [22]. This capability is primarily attributed to their layered structure and the use of non-linear activation functions such as the sigmoid, hyperbolic tangent, or ReLU functions, which empower these networks to encapsulate and model the complex, non-linear relationships intrinsic to real-world data. Mathematically, the computation within an MLP proceeds through the network layer by layer. Each neuron transforms its input through a weighted sum followed by a non-linear activation, mathematically described as:

$$a_i^l = \sigma\left(\sum_j w_{ij}^l a_j^{l-1} + b^l\right)$$

where a_i^l is the activation of the i-th neuron in the l-th layer, σ denotes the activation function, w_{ij}^l denotes the weight from the j-th neuron in the $(l-1)$-th layer to the i-th neuron in the l-th layer, and b^l is the bias term. The learning process, known as backpropagation, includes calculating the gradient of a loss function (characteristically mean squared error for regression or cross-entropy for classification tasks) with respect to the weights and biases, and repeatedly correcting these parameters to minimize the loss. This optimization is frequently achieved using gradient descent or its variants. Using this iterative learning process, MLPs can discern and observe the underlying structure of the training data. In the proposed control scheme, data is generated from PI controllers in both the voltage and current control loop to train the neural networks for each loop, then data is allocated for training, validation, and testing process (70% data for training, 15% for validation and 15% for testing) and the Levenberg-Marquardt algorithm available in MATLAB's Neural Network Toolbox is a method for training ANN. It is possible to specify a hidden layer with 10 neurons, while creating a network structure where the input data is processed through 10 intermediate nodes (neurons) that can capture complex patterns and relationships in the data before outputting the final prediction. This algorithm adjusts the weights of the network in a way that minimizes the difference between the predicted outputs and the actual outputs, efficiently finding solutions that might be difficult with other algorithms due to its approach that combines aspects of both the gradient descent and the Gauss-Newton methods, and the trainlm function in MATLAB's Neural Network Toolbox refers to a specific algorithm (Levenberg-Marquardt algorithm) used for training ANNs. It's particularly suited for networks involved in function fitting, or regression tasks, because of its efficiency and speed in finding solutions, especially in medium-sized and smaller problems where the computational overhead is manageable.

A. Voltage Control Loop

To achieve better dynamic response and for compensate the phase shifts as well as reactive power, an angular frequency, which results from a phase-locked loop, is utilized for cross-coupling to Vd and Vq. This is achieved by cross multiplication of with Vd to adjust Vq and vice versa. This approach not only aims at voltage regulation but also implicitly controls the reactive power, thereby enhancing the system's overall stability and performance under dynamic conditions. In this way, the current reference is generated in this loop in dq0 reference frame as in Equation (12) and Equation (13).

$$I_{d,Ref} = K_p(\Delta v_d - \omega v_q) + K_i \int (\Delta v_d - \omega v_q)dt \quad (12)$$

$$I_{q,Ref} = K_p(\Delta v_q + \omega v_d) + K_i \int (\Delta v_q + \omega v_d)dt \quad (13)$$

The data curation is performed in voltage control loop of PI-based controllers to acquire data for artificial neural networks. Then the voltage control loop of PI-based control scheme is modified for function fitting neural network, and data is obtained, trained, and finally implemented in Simulink, as can be observed in Fig. 2.

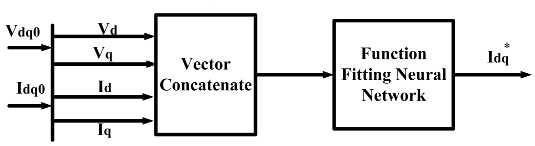

Fig. 2: Voltage Control Loop implemented in Simulink

B. Current Control Loop

The current control loop is designed to generate a reference voltage in dq0 frame. The current error across both dq-axis is calculated using Equation (14) and Equation (15).

$$\Delta i_d = I_{d,Ref} - i_d \quad (14)$$

$$\Delta i_q = I_{q,Ref} - i_q \quad (15)$$

The dynamic performance of this loop is enhanced by including cross coupling terms in the current error signals. These coupling terms can be observed in Equation (16) and Equation (17).

$$V_{d,com} = K_p(\Delta i_d + \omega L i_q) + K_i \int (\Delta i_d + \omega L i_q)dt \quad (16)$$

$$V_{q,com} = K_p(\Delta i_q - \omega L i_d) + K_i \int (\Delta i_q - \omega L i_d)dt \quad (17)$$

In the current control loop, data is achieved at these points using PI controllers to design ANN-based control scheme as shown in Fig. 3. Then finally PWM signals are generated to control the MOSFETs of three phase two- VSIs as can be observed in Fig. 4.

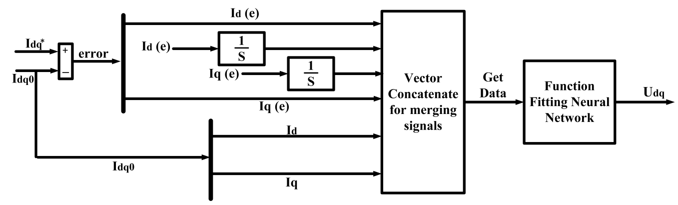

Fig. 3: Current Control Loop implemented in Simulink

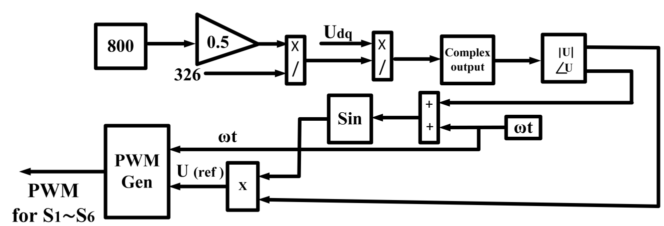

Fig. 4: Generation of PWM for three Phase VSI

IV. SIMULATION RESULTS AND DISCUSSIONS

The AC MG simulated in stand-alone operation is shown in Fig. 5. Initially, a purely resistive load of 7.5 kW is connected, and later on, another load resistive inductive (RL) load of 5 kVAR is introduced to observe the behavior of ANN during load or power transition to verify the robustness of the control scheme. The equivalent series resistance of the inductor is denoted by RL in Fig 5. The properly designed LC filter of the three-phase VSI helps improve power quality compliance with grid standards and ensure the reliable operation of different types of connected loads on the output side. The parameters used in simulation of AC MGs are given in Table II.

TABLE II: PARAMETERS USED IN AC MG

Parameter Name	Value	Unit
Input voltage	800	V
Inductance	10×10^{-3}	H
Equivalent series resistance of inductor	9×10^{-3}	Ω
Capacitance	16×10^{-6}	F
Resistive load	7.5	kW
Resistive inductive load	7.5, 5	kW ,kVAr
Sampling time	2×10^{-6}	Second
System frequency	50	HZ
Output voltage	326	V

A. Analysis of Purely Resistive Load under Steady-State Conditions

When a purely resistive load is connected at the PCC of AC MG at a frequency of 50 Hz. The output voltage of the system is maintained at 326 Volts and current is provided according to the load requirement. The simulation results for output voltage and current are shown in Fig. 6. It can be observed that ANN

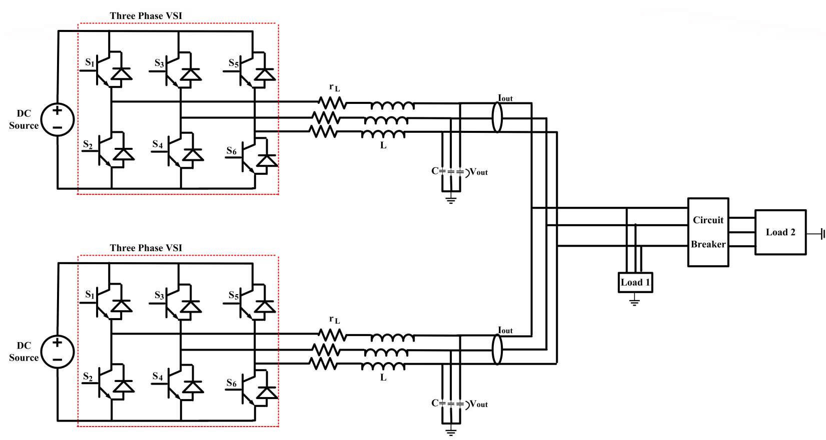

Fig. 5: Standalone AC MG with resistive load and RL load

based controller is working fine for AC MG and output voltage and current are smooth and stable in Fig. 6 The output power for resistive load can be observed in Fig. 6, which is also quite stable and smooth. Since it is a purely resistive load, reactive power is zero as shown in Fig. 6. In a purely resistive circuit, voltage and current are completely in phase so the phase difference is 0 degrees; therefore, reactive power is 0 in this case.

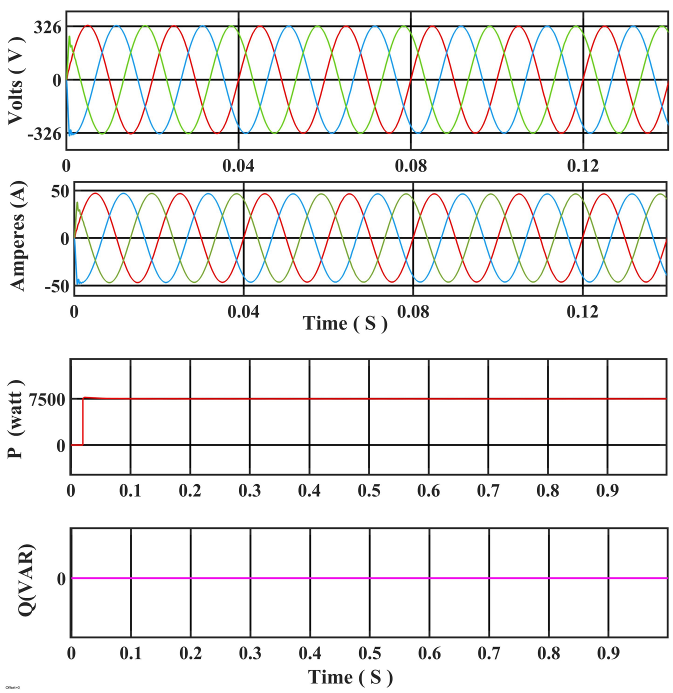

Fig. 6: Output voltage, current and power with resistive load

B. Simulation Results with Load Transitions

After 1 second, another load (RL load) is connected in parallel to the existing resistive load. The behavior of the controller for output voltage can be observed in Fig 7. Fig 7 shows that the controller can handle load variations quickly and provides stable output voltages. The output voltage behavior and output current with two loads (resistive load and RL load) are displayed in Fig. 7. After 2 seconds, the RL load is again disconnected to observe the controller response, and its robustness is confirmed, and AC MG is able to provide sinusoidal output voltages and currents, as shown in Fig. 7. The output power and its transitions during different load scenarios can be observed in Fig 8. Initially, a purely resistive load of 7.5 kW was connected and AC MG is providing the required power to meet the load demand. After 2 second, the RL load was disconnected from the AC MG and controller handles these load variations quickly. Thus, it is clear from the Fig. 7 that proposed ANN based controllers of AC MG are able to handle these load transitions in a stable and smooth way. The current and voltage THD value is according to internationals standards and grid codes and the values of both the THDs is 0.71% as can be seen in Fig. 8. In short, simulation results prove the robustness of control proposed strategy for analysing the performance of ANN based VSIs.

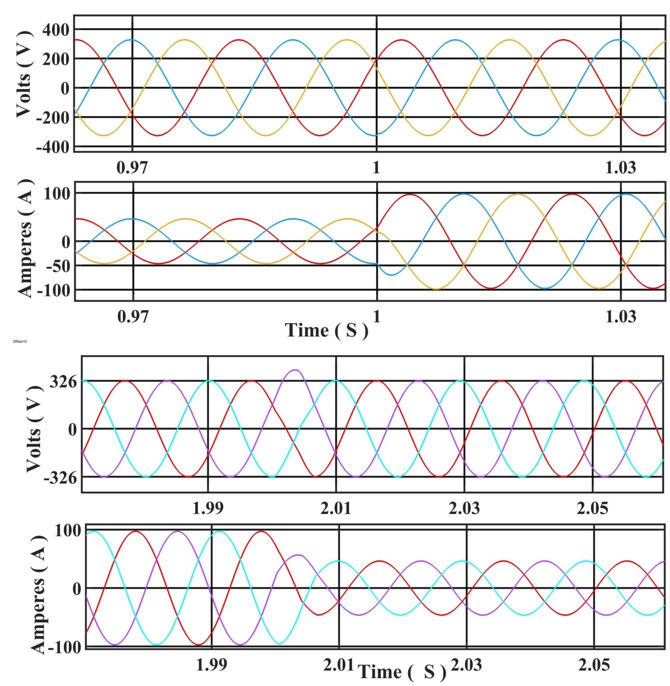

Fig. 7: Output voltage, current and power with resistive load and RL load during load transitions

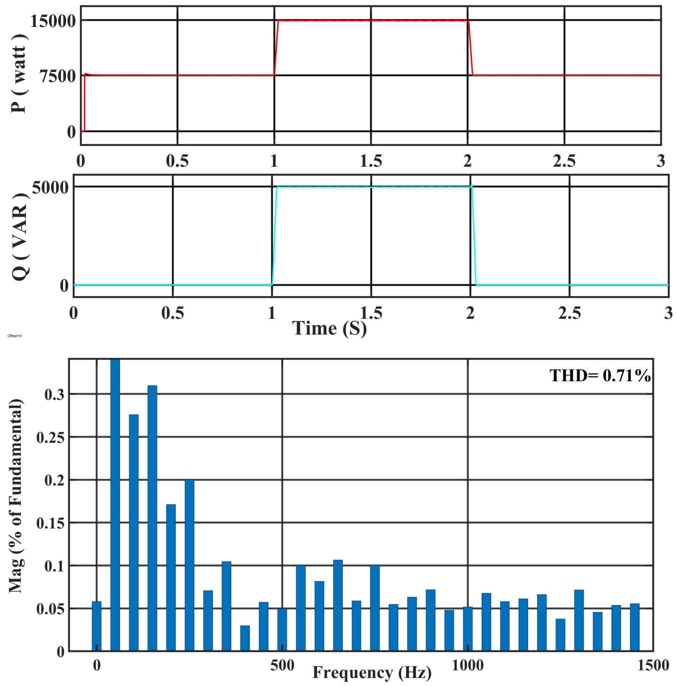

Fig. 8: Power Transitions in different load scenarios and THD of current/voltage in AC MG in standalone operations

V. CONCLUSION

This research paper proposes an ANN-based control approach for stand-alone operation of VSIs. The ANN-based controller is developed and trained in Simulink. To assess the efficacy of this control scheme, the ANN-based controller was trained and tested for varying load conditions. The voltage THD is only 0.71 % for stand-alone AC MG based on ANN controllers. The simulation results illustrate that the ANN-based controller consistently performs well in different load transitions while maintaining stable output voltages, thus confirming the robustness. In future, ANN based control strategy for grid-following VSIs can be developed.

VI. ACKNOWLEDGMENT

We extend our heartfel gratitude to the International Exchange Agreement between the University of Vaasa (Finland) and the Federal University of Uberlândia (Brazil), as well as the sponsorship of the Coordenacão de Aperfeiçoamento de Pessoal de Nível Superior - Brasil (CAPES) for their support for an international exchange visiting program. The assistance provided by CAPES has been instrumental in facilitating our research and academic endeavors at the University of Vaasa.

VII. REFERENCE

[1] Guerrero, Josep M., José Matas, L. Garcia De Vicunagarcia De Vicuna, Miguel Castilla, and Jaume Miret. ”Wireless-control strategy for parallel operation of distributed-generation inverters.” IEEE Transactions on Industrial Electronics 53, no. 5 (2006): 1461-1470.

[2] M. H. Saeed, W. Fangzong, B. A. Kalwar, and S. Iqbal, “A Review on Microgrids’ Challenges amp; Perspectives,” IEEE Access, vol. 9, pp. 166502–166517, 2021, doi: 10.1109/ACCESS.2021.3135083.

[3] R. Teodorescu, M. Liserre, and P. Rodríguez, “Islanding Detection,” Grid Convert. Photovolt. Wind Power Syst., pp. 93–122, 2011, doi: 10.1002/9780470667057.ch5.

[4] J. Hahn and T. F. Edgar, “Process Control Systems,” in Encyclopedia of Physical Science and Technology, vol. 2, Elsevier, 2003, pp. 111–126. doi: 10.1016/B0-12-227410-5/00612-8.

[5] K. H. Ang, G. Chong, and Y. Li, “PID control system analysis, design, and technology,” IEEE Trans. Control Syst. Technol., vol. 13, no. 4, pp. 559–576, 2005, doi: 10.1109/TCST.2005.847331.

[6] P. A. R. Freitas, L. P. Pires, L. C. Freitas, G. B. Lima, and L. C. G. Freitas, “Design and Development of a Grid-Tied PV Inverter With GMPPT Technique and Reduced Number of Sensors,” IEEE Access, vol. 10, pp. 48810–48823, 2022, doi: 10.1109/ACCESS.2022.3172404.

[7] P. Unruh, M. Nuschke, P. Strauß, and F. Welck, “Overview on grid-forming inverter control methods,” Energies, vol. 13, no. 10, 2020, doi: 10.3390/en13102589.

[8] R. H. PARK, “Two-Reaction Theory of Synchronous Machines: Generalized Method of Analysis-Part I,” Trans. Am. Inst. Electr. Eng., vol. 48, no. 3, pp. 716–727, 1929, doi: 10.1109/T-AIEE.1929.5055275.

[9] M. J. Mnati, D. V. Bozalakov, and A. Van den Bossche, “PID Control of a Three Phase Photovoltaic Inverter Tied to a Grid Based on a 120-Degree Bus Clamp PWM,” IFAC-PapersOnLine, vol. 51, no. 4, pp. 388–393, 2018, doi: 10.1016/j.ifacol.2018.06.097.

[10] H. Cha, T. K. Vu, and J. E. Kim, “Design and control of proportional-resonant controller based Photovoltaic power conditioning system,” 2009 IEEE Energy Convers. Congr. Expo. ECCE 2009, pp. 2198–2205, 2009, doi: 10.1109/ECCE.2009.5316374.

[11] S. Ul Islam et al., “Design of a proportional resonant controller with resonant harmonic compensator and fault ride trough strategies for a grid-connected photovoltaic system,” Electron., vol. 7, no. 12, 2018, doi: 10.3390/electronics7120451.

[12] H. S. Khan, I. S. Mohamed, K. Kauhaniemi and L. Liu, ”Artificial Neural Network-Based Voltage Control of DC/DC Converter for DC Microgrid Applications,” 2021 6th IEEE Workshop on the Electronic Grid (eGRID), New Orleans, LA, USA, 2021, pp. 1-6, doi: 10.1109/eGRID52793.2021.9662132.

[13] H. M. Hasanien and M. Matar, “A fuzzy logic controller for autonomous operation of a voltage source converter-based distributed generation system,” IEEE Trans. Smart Grid, vol. 6, no. 1, pp. 158–165, 2015, doi: 10.1109/TSG.2014.2338398.

[14] H. O. Omotoso et al., “Machine Learning Supervisory Control of Grid-Forming Inverters in Islanded Mode,” Sustain., vol. 15, no. 10, 2023, doi: 10.3390/su15108018.

[15] Chi-Huang Lu, “Design and Application of Stable Predictive Controller Using Recurrent Wavelet Neural Networks,” IEEE Trans. Ind. Electron., vol. 56, no. 9, pp. 3733–3742, Sep. 2009, doi: 10.1109/TIE.2009.2025714.

[16] Shuzhi Sam Ge, Chenguang Yang, and Tong Heng Lee, “Adaptive Predictive Control Using Neural Network for a Class of Pure-Feedback Systems in Discrete Time,” IEEE Trans. Neural Networks, vol. 19, no. 9, pp. 1599–1614, Sep. 2008, doi: 10.1109/TNN.2008.2000446.

[17] A. F. Gad and F. E. Jarmouni, “Introduction to artificial neural networks (ANN),” Introd. to Deep Learn. Neural Networks with PythonTM, pp. 15–32, 2021, doi: 10.1016/b978-0-323-90933-4.00007-3.

[18] S. Yarikkaya and K. Vardar, “Neural Network Based Predictive Current Controllers for Three Phase Inverter,” IEEE Access, vol. 11, no. February, pp. 27155–27167, 2023, doi: 10.1109/ACCESS.2023.3258679.

[19] M. Demirtas, I. Cetinbas, S. Serefoglu, and O. Kaplan, “ANN controlled single phase inverter for solar energy systems,” 16th Int. Power Electron. Motion Control Conf. Expo. PEMC 2014, pp. 768–772, 2014, doi: 10.1109/EPEPEMC.2014.6980590.

[20] M. Ali et al., “Robust ANN-Based Control of Modified PUC-5 Inverter for Solar PV Applications,” IEEE Trans. Ind. Appl., vol. 57, no. 4, pp. 3863–3876, 2021, doi: 10.1109/TIA.2021.3076032.

[21] H. S. Khan and K. Kauhaniemi, ”Design and FPGA-in-loop based validation of predictive hierarchical control for islanded AC microgrid,” Engineering Science and Technology, an International Journal, vol. 48, p. 101557, 2023.

[22] Kocer, Emir, Tsz Wai Ko, and J¨org Behler. ”Neural network potentials: A concise overview of methods.” Annual review of physical chemistry 73 (2022): 163-186.